

# Anchoring of Nematic Liquid Crystals on Viruses with Different Envelope Structures

Chang-Hyun Jang, Li-Lin Cheng,<sup>†</sup> Christopher W. Olsen,<sup>†</sup> and Nicholas L. Abbott\*

*Department of Chemical and Biological Engineering and Department of Pathobiological Sciences - School of Veterinary Medicine, University of Wisconsin, Madison, Wisconsin 53706*

Received March 21, 2006

## ABSTRACT

The ordering of synthetic liquid crystals near surfaces is known to be dependent on the nanoscopic structure and chemical functionality of surfaces. In this letter, we report that the orientational ordering of synthetic liquid crystals on surfaces decorated with viruses is also dependent on the structures of the viruses. Each of the four virions investigated had diameters of approximately 100 nm, but three of the viruses (influenza virus, La Crosse virus, and vesicular stomatitis virus) were enveloped in a lipid bilayer, whereas one virus (adenovirus) was not. We observed that lipid bilayer-enveloped viruses induce homeotropic (perpendicular) ordering of a nematic liquid crystal upon contact with the liquid crystal. In contrast, nonenveloped virus (adenovirus)-treated surfaces caused a near-planar orientation of the liquid crystal. We conclude that the homeotropic ordering of liquid crystals is a signature of the presence of enveloped viruses present on surfaces. These results suggest new approaches to the design of nanostructured materials that incorporate viruses as well as suggest methods that can be used to amplify the presence of nanoscopic virions into micrometer-sized domains of liquid crystal that can be optically probed.

This paper reports a study of the interactions of synthetic liquid crystals (LCs) and viruses supported on nanostructured surfaces. The study sought to understand how the structure of the virus impacts the orientational order within the contacting LC. The study is broadly motivated by the observation that understanding the interactions of synthetic LCs and viruses may provide new approaches to the design of materials that incorporate viruses as well as provide methods to report (sense) the presence of viruses. Because viruses can be engineered to present chemical functional groups with a high degree of precision in three dimensions, they provide useful building blocks for novel approaches to material fabrication.<sup>1,2</sup> Recent studies have also shown that LCs can be used to amplify and report the presence of a range of biological species displayed at surfaces through the orientations assumed by the LCs when in contact with the biological species.<sup>3,4</sup> LC-based reporting offers potential advantages over conventional techniques because it does not require complex instrumentation,<sup>5</sup> laborious techniques,<sup>6</sup> or enzymatic or fluorescent labels.<sup>7</sup>

In this study, we investigate the orientational behavior of the nematic phase of 4-cyano-4'-pentylbiphenyl (5CB) on surfaces presenting electrostatically bound viral particles that

possess different envelope structures. We demonstrated previously that the uniform planar alignment of 5CB on poly-L-lysine-treated gold films deposited by physical vapor deposition at an oblique angle of incidence is changed to a homeotropic (perpendicular) alignment by the presence of bound vesicular stomatitis viruses because of interactions that occur between the viral particles bound to these surfaces and the LCs.<sup>8</sup> The study we report in the present paper tests the hypothesis that the anchoring of LCs on surfaces presenting viruses is influenced by the external structures of viruses and, thus, may depend on the identity of the virions. Four different viruses [adenovirus (ADV), influenza virus (IFV), La Crosse virus (LACV), and vesicular stomatitis virus (VSV)] were chosen for the current study because they are comparable in physical dimensions (they are all roughly 100 nm in diameter) and yet present distinct structural differences, which are summarized in Table 1. The infectious VSV particle is bullet-shaped, IFV and LACV are approximately spherical in shape, and ADV is an icosahedron. Both IFV and VSV possess peripheral matrix proteins that lie between a phospholipid envelope and their nucleocapsid cores. For VSV, there are about 1800 molecules of the viral matrix proteins (26 KDa) per virion,<sup>9</sup> whereas IFV possesses about 3000 molecules per virion (27.8 KDa/protein).<sup>10</sup> LACV also possesses a lipid bilayer envelope, but LACV virions do not contain matrix protein. Because of the above structural

\* Corresponding author. Phone: (608) 265-5278. Fax: (608) 262-5434. E-mail: [abbott@engr.wisc.edu](mailto:abbott@engr.wisc.edu).

<sup>†</sup> Department of Pathobiological Sciences - School of Veterinary Medicine.

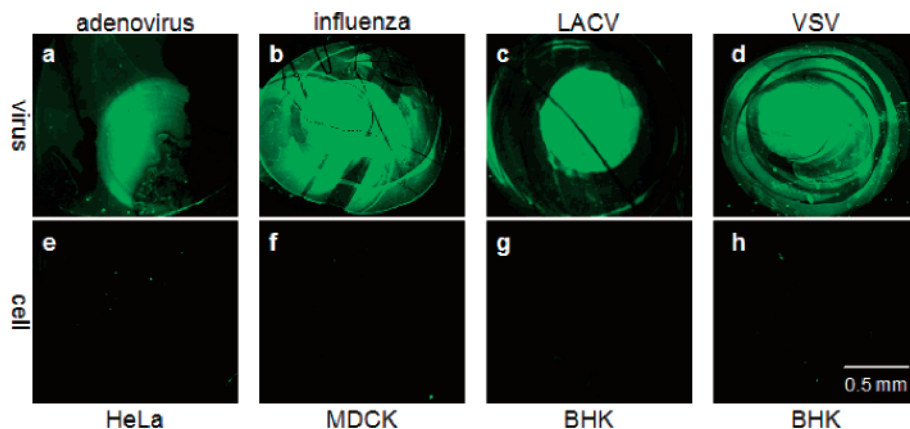


**Figure 1.** (a–d) Fluorescent micrographs of viruses that were captured by adsorption onto poly-L-lysine-treated surfaces. The images were obtained after incubation of the surfaces with antibodies specific to each virus and a secondary antibody (0.2 mM of FITC-conjugated goat anti-rabbit IgG or anti-chicken IgY antibody). The control experiments (e–h) used samples obtained from cell cultures that were not infected with viruses but subjected to the same sample preparation steps. In this study, adeno and influenza viruses were grown in HeLa and MDCK cells, respectively, and BHK cells were used to prepare LACV and VSV.

**Table 1.** Structural and Compositional Characteristics of Viruses Used in This Study<sup>20,21</sup>

	adenovirus <sup>22</sup>	influenza <sup>23</sup>	LACV <sup>24</sup>	VSV <sup>25</sup>
classification	Adenoviridae	Orthomyxoviridae	Bunyaviridae	Rhabdoviridae
size & morphology	70–100 nm icosahedron	80–120 nm in diameter	80–100 nm in diameter	75 × 180 nm bullet shape
nucleic acid (wt %)	13	1	2	1–2
protein (wt %)	87 (protein shell w/fiber)	70 (w/matrix protein)	58 (no matrix protein)	65–75 (w/matrix protein)
lipid envelope (wt %)	no membrane or lipid	20	33	15–25
carbohydrate (wt %)	trace	5–8	7	3
isoelectric range (pH)	5.5–6.3	6.5–7.0	6.7–8.4	4.7–7.0

differences, the membranes of IFV and VSV are believed to be more rigid than LACV. ADV has neither a lipid membrane nor matrix protein.

First, we deposited poly-L-lysine onto the surfaces of gold films by contacting the surfaces with aqueous drops of 0.1% poly-L-lysine in a water-saturated environment. As described in detail in our previous studies,<sup>11</sup> we prepared the gold films with an anisotropic surface structure by physical vapor deposition of gold onto glass substrates at an oblique angle of incidence. Because of self-shadowing, the nanometer-scale roughness of the gold surface is greatest in an azimuthal direction that is parallel to the plane of incidence of the gold during deposition of the film. A past study using atomic force microscopy has shown that the characteristic size of the grains within the polycrystalline gold film is ~14 nm and the difference in height between hills and valleys defined by the grains is ~2 nm when the gold is deposited at an angle of incidence of 60° (measured from normal).<sup>12</sup> After 30 min of incubation with the poly-L-lysine, the gold surfaces were rinsed with water and dried under a stream of N<sub>2</sub>. We sought to immobilize the viruses on these cationic surfaces by electrostatic interactions between the viruses and cationic surfaces. On the basis of the known isoelectric ranges of the viruses (determined by electrokinetic studies), all four viruses have a net negative surface charge in the STE buffer (pH 8.0) used in this study (See Table 1).<sup>13–15</sup> We note that the focus of this paper is on the nature of the coupling between the LC and viruses; we do not seek to achieve a

selective capture of each virus from a complex mixture on the surface. As described below, our experiments are performed with purified viruses.

We initially confirmed binding of the viruses to the poly-L-lysine surface by using fluorescently labeled antibodies. The virus samples used in this study were purified through a buoyant density gradient and centrifugation to remove cell debris (see below for control experiments). Viruses were diluted in STE buffer to obtain titers of  $2 \times 10^8$  pfu/mL, and then 5  $\mu$ L droplets of each dispersion of virus were incubated on the poly-L-lysine surfaces for 1 h in a humid environment. After incubation, the unbound virus particles were rinsed from the surface with sterile double-distilled water (rinsing was performed twice) and the surface was dried under a stream of air. The virus-decorated slide was immersed in a 0.1% (by weight) solution of bovine serum albumin (BSA) before applying primary antibodies specific to each type of virus. After washing twice with water and drying the surface, FITC-conjugated goat anti-rabbit IgG or anti-chicken IgY antibodies were applied for 1 h at room temperature. The slide was then washed three times before imaging was performed by using a fluorescence microscope. Figure 1a–d shows fluorescent micrographs of these virus-decorated surfaces. Inspection of Figure 1a–d reveals the presence of circular domains of high fluorescence intensity. The circular domains correspond to the areas of contact between the surfaces and the droplets containing the virus particles. The concentric rings result from evaporation of the

**Table 2.** Quantitation of Viruses Adsorbed on Poly-L-lysine Surfaces<sup>a</sup>

	adenovirus	influenza	LACV	VSV
titer of virus in droplet placed onto surface (pfu/ml)	$2.0 \times 10^8$	$2.0 \times 10^8$	$2.0 \times 10^8$	$2.7 \times 10^8$
amount of virus in droplet placed onto surface (pfu)	$1.0 \times 10^6$	$1.0 \times 10^6$	$1.0 \times 10^6$	$1.35 \times 10^6$
amount of virus not bound to surface (pfu)	$1.5 \times 10^5$	$1.0 \times 10^5$	$0.6 \times 10^5$	$1.5 \times 10^5$
amount of virus bound to surface (pfu)	$8.5 \times 10^5$	$9.0 \times 10^5$	$9.4 \times 10^5$	$12 \times 10^5$
ellipsometric thickness of bound virus (nm) $2 \times 10^8$ pfu/ml	$17.0 \pm 3.8$	$14.0 \pm 0.5$	$17.3 \pm 2.4$	$14.5 \pm 0.8$
ellipsometric thickness of bound virus (nm) $2 \times 10^7$ pfu/ml	$4.4 \pm 1.6$	$3.3 \pm 0.4$	$3.3 \pm 0.8$	$1.3 \pm 0.3$

<sup>a</sup> The optical thickness reported in Table 2 is the average of two samples, each sample measured at three different points.

droplets during the incubation of virus solutions on the surfaces (the domains are not exactly circular because of the effects of blow drying the surfaces with a stream of air). We also performed control experiments using samples obtained from cell cultures that were not infected with viruses but subjected to the same sample preparation steps described above (centrifugation, etc). The control experiments did not lead to the formation of the bright circular domains seen using preparations from virus-infected cells (Figure 1e–h). Thus, we conclude that the bright domains (Figure 1a–d) are the result of the recruitment and binding of FITC-labeled antibodies to the surface-bound viruses and that each of the four viruses was captured on the poly-L-lysine-decorated surfaces.

Although the experiments described above provide qualitative evidence for the presence of each type of virus on the surfaces, we performed two additional experiments to quantify the amount of each virus captured. First, we incubated 5  $\mu$ L droplets of each virus on the poly-L-lysine surfaces for 2 h in a humid environment. Following the 2 h incubation, the droplets were removed from the surface using a pipet and placed into a tube along with a buffer that was used to rinse the surface. A control sample containing a 5  $\mu$ L droplet of each virus was simultaneously incubated at room temperature for 2 h (not on the surface). We then determined the number of plaque-forming units of virus in each sample removed from the surface and by difference calculated the amount of virus bound to the surface (Table 2). The results in Table 2 show that ADV, IFV, and LACV were present at  $8.5 \times 10^5$ ,  $9.0 \times 10^5$ , and  $9.4 \times 10^5$  pfu, respectively. The pfu of VSV bound to the surface was slightly higher ( $12 \times 10^5$  pfu) than the other three viruses because of the higher number of pfu of VSV incubated on the surface in these experiments (see Table 2). We note that the fraction of all four viruses captured on the surfaces from the droplets is very similar ( $90 \pm 5\%$ ). Second, we measured the ellipsometric thickness of the virions bound to the surfaces using the procedure described above. Prior to measurement of the ellipsometric thickness, the surfaces were rinsed with sterile double-distilled water and dried under a stream of air. Inspection of Table 2 reveals that similar ellipsometric thicknesses were recorded for each virus, and the ellipsometric thickness was observed to decrease with the titer of the virus in solution incubated on the surface. These results, when combined, support our conclusion that incubation of droplets of ADV, IFV, LACV, or VSV (same titer) leads to surfaces that are decorated with similar amounts (pfu and ellipsometric thickness) of each of the four viruses.

Next, we investigated the orientational behavior of 5CB on the virus-decorated surfaces. Using a procedure similar to that described above, we placed droplets of each virus solution of titer  $2 \times 10^8$  pfu/mL on a poly-L-lysine surface and incubated the surface in a water-saturated environment for 2 h. The surface was then rinsed with water and dried under a stream of N<sub>2</sub>. We contacted LC with the surface by using an optical cell that was fabricated by pairing a surface of interest and an octyltrichlorosilane-treated glass slide. The two surfaces were spaced apart by placing Saran Wrap (thickness of  $\sim 13 \mu\text{m}$ ) at the edges of the surfaces and secured by binding clips. 5CB was then introduced into the cavity between the two surfaces by using capillary forces at a temperature (35–40 °C) corresponding to the isotropic state of 5CB. The sample was cooled, and the optical appearances of the nematic LC films were recorded at room temperature by using polarized light microscopy (white light, transmission mode).

Figure 2 shows the optical appearance of nematic LC (cross polars) in contact with surfaces presenting the four different viruses. Inspection of Figure 2a reveals a largely dark optical texture with line defects (bright lines) and a small pink region on the ADV-laden surface when the sample was oriented with the direction of gold deposition parallel to either of the polarizers. Upon rotation of the sample by 45°, the optical texture turned bright, with the color of the LC in contact with the virus-coated domain being slightly different from the color of the surrounding poly-L-lysine-coated surface (Figure 2e). This difference in interference color indicates that the 5CB on the region of the surface decorated with ADV is tilted away from the surface relative to the region of the surface coated with only poly-L-lysine. Past studies have demonstrated that it is possible to quantitatively evaluate the tilt angle of a LC at a surface from knowledge of the interference color, optical properties of LC, and the geometry of a sample.<sup>16</sup> Our analysis of the interference colors in Figure 2e revealed that ADV causes 5CB to tilt away from the surface by approximately 10°.

We observed uniformly dark textures on surfaces presenting IFV, LACV, or VSV (Figure 2b–d). Upon rotation by 45°, these surfaces showed no modulation of the intensity of transmitted light, suggesting homeotropic alignment of 5CB (Figure 2f–h). Homeotropic alignment of LC on these surfaces was confirmed by conoscopy (inset in Figure 2f–h). We note that the nonhomeotropic regions inside the homeotropic circles in Figure 2b, d, f, and h are the result of damage to the surface caused by contact of the pipet tip with the surface during the spotting of virus solution.

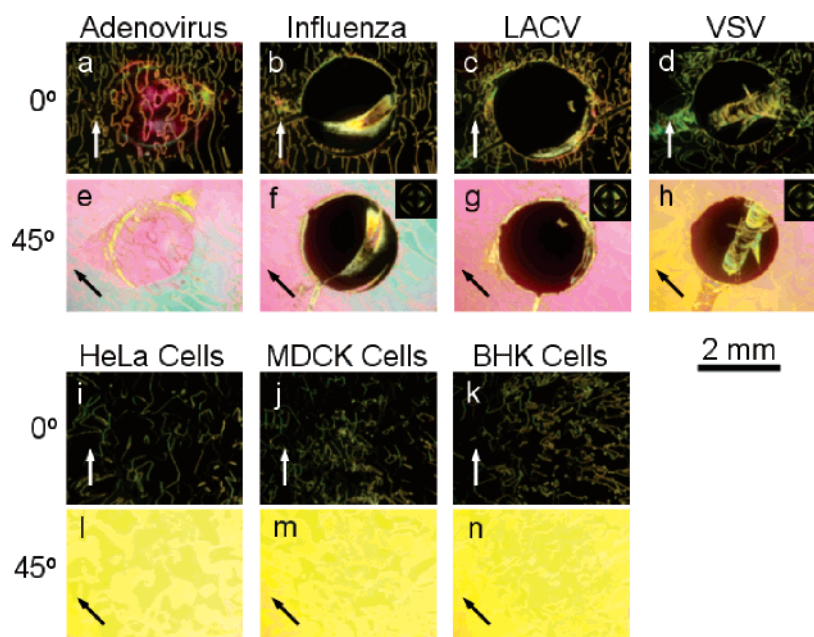


**Figure 2.** Optical images (crossed polars) of nematic 5CB sandwiched in an optical cell composed of two surfaces. The first surface comprised a poly-L-lysine-treated gold film (obliquely deposited) that was contacted with a droplet of virus solution or a negative control solution (cell supernatant, cells not infected with viruses) for 2 h. The second surface was octyltrichlorosilane-treated glass. The circular domains in a–h were caused by the contact of the poly-L-lysine surfaces with the virus solutions (titer of  $2 \times 10^8$  pfu/mL). The arrow in each image indicates the direction of deposition of gold. The samples were oriented such that the direction of deposition of the gold film was oriented at an angle of  $0^\circ$  (a–d, i–k) or  $45^\circ$  (e–h, l–n) from one of the polarizers. The insets correspond to conoscopic images of the samples (f–h). All images were obtained immediately after the assembly of the liquid crystal cell.

To confirm that the above-described orientations of the LCs were due to the presence of the virus and not, for example, due to the presence of cell debris that had passed through the purification steps, we prepared samples using the same procedures described above except that supernatant from uninfected cells was used. None of the control samples induced homeotropic alignment and/or caused any measurable difference in the orientation of the LC between the region spotted with the control sample and the surrounding poly-L-lysine-coated region (Figure 2i–n). These results support our conclusion that the orientations of LCs observed on the surfaces on which virus was applied is due to the bound virions and not cell debris associated with the virions. Finally, we also performed control experiments in which we incubated the poly-L-lysine-coated gold surfaces in STE buffer for 2 h, rinsed the surfaces with water, and then dried the surfaces under a stream of  $N_2$ . By examination with crossed polarizers, we concluded that incubation of the sample under STE did not change the orientation of the LC (data not shown).

The results above, when combined, support the hypothesis that the homeotropic alignment of 5CB observed on surfaces decorated with IFV, LACV, and VSV is due to the lipid envelope of the viruses. This homeotropic anchoring contrasts with the near-planar alignment of 5CB on nonenveloped virus (ADV)-laden surfaces. Our control experiments revealed that neither the cell debris remaining in the virus sample nor the buffering salts cause the homeotropic alignment of 5CB.

Because the three viruses (VSV, LACV, and IFV) that are surrounded by a phospholipid membrane cause homeotropic anchoring of a nematic LC, our results suggest that

the physical interaction between the lipid coat of the virus and the LC (e.g., penetration of 5CB into the lipid membrane bilayers surrounding virus particles) leads to the homeotropic alignment of 5CB on these surfaces. Although it is possible that the packing (spatial arrangement) and orientation of the virions may also influence the ordering of the LC, we note here that the maximal surface densities of virions used in our studies correspond to 1 virion per  $10 \mu\text{m}^2$  and that the virions are therefore not close packed on these surfaces. We also note that IFV, VSV, and LACV have different shapes (see Table 1), yet they give rise to the same orientation of the LCs. This observation leads us to conclude that it is unlikely that the orientation of the viruses on the surfaces underlie the two different orderings of the LCs observed on enveloped and nonenveloped viruses.

Several additional observations provide further support for our proposition that the lipid envelope of the viruses leads to the homeotropic orientation of the LC. First, tilted or homeotropic anchoring of 5CB on surfaces supporting biological materials, such as cells and phospholipid monolayers, has been reported (although we note that the surface of a cell presents a range of proteins and carbohydrates that may also interact with LC).<sup>17,18</sup> Second, we have also reported that mixed self-assembled monolayers formed from *n*-alkanethiols with long ( $\text{CH}_3(\text{CH}_2)_{15}\text{SH}$ ) and short ( $\text{CH}_3(\text{CH}_2)_4\text{SH}$ ) or aliphatic  $\text{CH}_3(\text{CH}_2)_9\text{SH}$ ) chains can homeotropically anchor nematic phases of 5CB or *p*-methoxybenzylidene-*p*-*n*-butylaniline (MBBA).<sup>19</sup> When the SAMs have a low density of long aliphatic chains, LCs can penetrate into the monolayer, which results in the homeotropic anchoring of nematic phases.

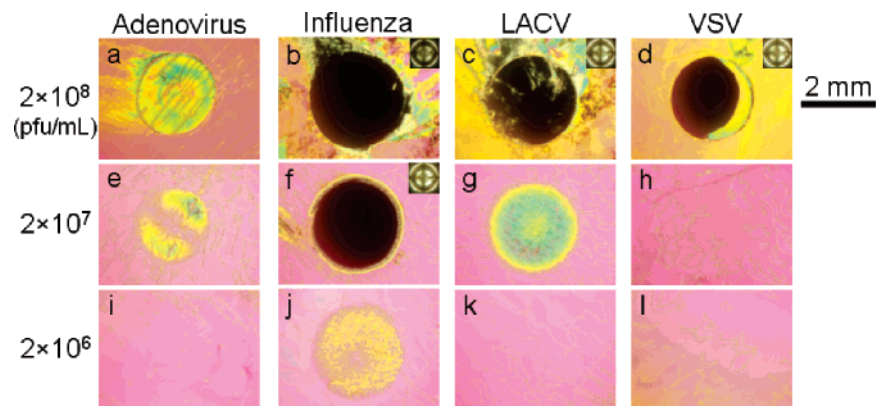


**Figure 3.** Optical images (crossed polars) of 5CB sandwiched in an optical cell composed of two surfaces. The first surface comprised a poly-L-lysine-treated gold film (obliquely deposited) that was contacted with a droplet of virus solution for 2 h at different concentrations. The second surface was octyltrichlorosilane-treated glass. The numbers on the left side of the LC images represent the concentrations of the virus solutions. The circular domains shown in the optical images were caused by the contact of the poly-L-lysine surfaces with the virus solutions. The samples were oriented such that the direction of deposition of the gold film was oriented at an angle of  $45^\circ$  from one of the polarizers. The insets correspond to conoscopic images of the samples (b–d, f). All images were obtained immediately after the assembly of the liquid crystal cell.

Finally, we decreased the concentrations (titers) of viruses in the solutions incubated on the surfaces to provide an estimate of the number density of viruses on surfaces that cause the homeotropic orientation of the LCs (Figure 3). We prepared virus solutions with three different titers ( $2 \times 10^8$ ,  $2 \times 10^7$ , and  $2 \times 10^6$  pfu/mL) and incubated them on poly-L-lysine surfaces as described above. Inspection of Table 2 reveals that dilution of the viruses from  $2 \times 10^8$  to  $2 \times 10^7$  pfu/mL leads to a decrease in the ellipsometric thickness of virus on each surface. Observation of optical cells fabricated with surfaces treated with virus solutions of titer  $2 \times 10^8$  pfu/mL revealed the optical texture similar to that in Figure 2: homeotropic anchoring of 5CB for the surfaces presenting IFV, VSV, or LACV (Figure 3b–d) and near planar alignment for the surface presenting ADV (Figure 3a). However, when the samples were incubated with virus solutions of titer  $2 \times 10^7$  pfu/mL, only the IFV sample induced homeotropic anchoring and the rest of the samples showed planar or near-planar alignment of 5CB (Figure 3e–h). When we further diluted the virus solutions 10-fold ( $2 \times 10^6$  pfu/mL), the anchoring of 5CB on all 4 surfaces were planar or slightly tilted (Figure 3i–l). We estimated the upper limit on the number density of virions on the surface giving rise to the response in Figure 3f to be  $\sim 1$  virion/ $100 \mu\text{m}^2$  by assuming that all virions in the solution adsorb on the poly-L-lysine surface (see Table 2). Because LCs can be used to image regions of surfaces that are  $\sim 100 \mu\text{m}^2$ , this results suggests that it may be possible to image single virions or small clusters of virions on the surfaces reported in this paper by using nematic LCs.

In summary, we have found that surfaces that present three viruses (IFV, LACV, or VSV) with lipid envelopes cause homeotropic alignment of a nematic LC. In contrast, ADV, a virus that does not possess a lipid envelope, causes near-planar alignment of the LC. Thus, homeotropic ordering of the LC appears to be a signature of the presence of enveloped viruses. These results suggest that LCs may provide routes to reporting the presence of viruses captured on surfaces (e.g.,

diagnostics for emerging diseases or biosecurity) and that interactions exist between enveloped viruses and synthetic LCs which might find use in novel approaches to materials synthesis that exploit viruses as building blocks.

**Acknowledgment.** This research was partially supported by the National Science Foundation (DMR 0520527, BES 0330333, CTS-040815) and the National Institutes of Health (R01 CA108467-01). Barbara Israel is thanked for helpful comments.

**Supporting Information Available:** Please see the Supporting Information for experimental details describing cell culture, purification of viruses, determination of titer, oblique deposition of gold, treatment of glass slides with octyltrichlorosilane, and optical examination of LCs. This material is available free of charge via the Internet at <http://pubs.acs.org>.

## References

- (1) Douglas, T.; Young, M. *Nature* **1998**, *393*, 152.
- (2) Lee, S.-W.; Mao, C.; Flynn, C. E.; Belcher, A. M. *Science* **2002**, *296*, 892.
- (3) Gupta, V. K.; Skaife, J. J.; Dubrovsky, T. B.; Abbott, N. L. *Science* **1998**, *279*, 2077.
- (4) Luk, Y.-Y.; Tingey, M. L.; Hall, D. J.; Israel, B. A.; Murphy, C. J.; Bertics, P. J.; Abbott, N. L. *Langmuir* **2003**, *19*, 1671.
- (5) Pandey, A.; Mann, M. *Nature* **2000**, *405*, 837.
- (6) Venien, A.; Levieux, D.; Dufour, E. *J. Colloid Interface Sci.* **2000**, *223*, 215.
- (7) Nielsen, U. B.; Cardone, M. H.; Sinskey, A. J.; MacBeath, G.; Sorger, P. K. *Proc. Natl. Acad. Sci. U.S.A.* **2003**, *100*, 9330.
- (8) Tercero Espinoza, L. A.; Schumann, K. R.; Luk, Y.-Y.; Israel, B. A.; Abbott, N. L. *Langmuir* **2004**, *20*, 2375.
- (9) Rose, J. K.; Whitt, M. A. Rhabdoviridae: The viruses and their replication. In *Fields Virology*; Knipe, D. M., Howley, P. M., Eds.; Lippincott Williams & Wilkins Press: Philadelphia, PA, 2001; Vol. I, p 1221–1224.
- (10) Lamb, R. A.; Krug, R. M. Orthomyxoviridae: The viruses and their replication. In *Fields Virology*; Knipe, D. M., Howley, P. M., Eds.; Lippincott Williams & Wilkins Press: Philadelphia, PA, 2001; Vol. I, p 1487–1490.
- (11) Gupta, V. K.; Abbott, N. L. *Langmuir* **1996**, *12*, 2587.

- (12) Skaife, J. J.; Brake, J. M.; Abbott, N. L. *Langmuir* **2001**, *17*, 5448.
- (13) Nasz, I.; Lengyel, A.; Adaam, E.; Medveczky, P. *Virology* **1977**, *28*, 117.
- (14) Bosch, F. X. *Arch. Virol.* **1985**, *83*, 311.
- (15) Miki, T. *Microbiol. Immunol.* **1981**, *25*, 585.
- (16) Brake, J. M.; Mezera, A. D.; Abbott, N. L. *Langmuir* **2003**, *19*, 8629.
- (17) Brake, J. M.; Daschner, M. K.; Luk, Y.-Y.; Abbott, N. L. *Science* **2003**, *302*, 2094.
- (18) Fang, J.; Ma, W.; Selinger, J. V.; Shashidhar, R. *Langmuir* **2003**, *19*, 2865.
- (19) Drawhorn, R. A.; Abbott, N. L. *J. Phys. Chem.* **1995**, *99*, 16511.
- (20) Obijeski, J. F.; Murphy, F. A. *J. Gen. Virol.* **1977**, *37*, 1.
- (21) Compans, R. W.; Choppin, P. W. *Comprehensive Virology*; Plenum Press: New York, 1975; Vol. IV.
- (22) Green, M.; Pina, M. *Virology* **1963**, *20*, 199.
- (23) Compans, R. W.; Choppin, P. W. Reproduction of Myxoviruses. In *Comprehensive Virology*; Fraenkel-Conrat, H., Wagner, R. R., Eds.; Plenum Press: New York, 1975; Vol. IV, p 56–70.
- (24) Brockus, C. L.; Grimstad, P. R. *Virus Genes* **1999**, *19*, 73.
- (25) International committee on taxonomy of viruses database (ICTVdB). Descriptions of vesicular stomatitis Indiana virus can be found at <http://www.ictvdb.rothamsted.ac.uk/ICTVdB/62010001.htm>.

NL060625G